

SCIENTIFIC REPORTS



OPEN

Identification of *BnaYUCCA6* as a candidate gene for branch angle in *Brassica napus* by QTL-seq

Hui Wang*, Hongtao Cheng*, Wenxiang Wang, Jia Liu, Mengyu Hao, Desheng Mei, Rijin Zhou, Li Fu & Qiong Hu

Received: 17 February 2016
Accepted: 11 November 2016
Published: 06 December 2016

Oilseed rape (*Brassica napus* L.) is one of the most important oil crops in China as well as worldwide. Branch angle as a plant architecture component trait plays an important role for high density planting and yield performance. In this study, bulked segregant analysis (BSA) combined with next generation sequencing technology was used to fine map QTL for branch angle. A major QTL, designated as *branch angle 1* (*ba1*) was identified on A06 and further validated by Indel marker-based classical QTL mapping in an F₂ population. Eighty-two genes were identified in the *ba1* region. Among these genes, *BnaA0639380D* is a homolog of *AtYUCCA6*. Sequence comparison of *BnaA0639380D* from small- and big-branch angle oilseed rape lines identified six SNPs and four amino acid variation in the promoter and coding region, respectively. The expression level of *BnaA0639380D* is significantly higher in the small branch angle line Purler than in the big branch angle line Huyou19, suggesting that the genomic mutations may result in reduced activity of *BnaA0639380D* in Huyou19. Phytohormone determination showed that the IAA content in Purler was also obviously increased. Taken together, our results suggested *BnaA0639380D* is a possible candidate gene for branch angle in oilseed rape.

Rapeseed is one of the most important oil crops worldwide and yield enhancement is very important for achieving high production profit. As the arable lands gradually decrease due to growing population, high-density planting is a good approach for high efficiency of resource utilization^{1–3}. Among all the agronomic traits under domestication process, plant architecture, e.g. leaf angle or branch angle, has played an important role in the adaption to high-density planting at present⁴. Genetic gain of yield has been enhanced in some crops, especially in maize, through breeding for high-density tolerance^{2,3}. Therefore, optimized plant architecture suitable for high-density planting is regarded as one of the most important goals to improve the yield in oilseed rape, as well as in other cultivated crops.

Plant architecture is usually defined as the three-dimensional structure of aerial parts of plant, which is determined by plant height, branch pattern and number, leaf shape as well as morphology of other organs^{5–7}. Branch angle is one of the most important traits of plant architecture, as it determines the optimum planting density and influences yield through affecting photosynthesis efficiency⁸. Smaller leaf inclination angle in sorghum caused solar radiation to penetrate deeper into the canopy and is predicted to increase the biomass yield⁹. Erect leaf trait can enhance photosynthetic efficiency and allow for increased planting density, thus leading to higher grain yield in maize¹⁰. Tiller angle in rice has attracted interests since the past decades because of agronomic importance^{11,12}.

A multitude of results showed that tiller or leaf angle is a quantitative trait, which is mainly controlled by major genes and influenced by minor QTL. QTL/genes for tiller or leaf angle have been identified and investigated extensively. Some characterized genes shed lights on the mechanisms for the genetic control of leaf or tiller angle. In *Arabidopsis*, the auxin receptor mutant *tir1-1* has lateral branches that are less vertical¹³. *Indeterminate domain 15* (*Idd15*)/*shoot gravitropism 5* (*sgr5*) mutants displayed increased orientation angles in both branches and siliques¹⁴. *Tiller angle control1* (*TAC1*) and *LAZY1* were two important genes modulating rice tiller angle^{15,16}. *Loose Plant Architecture1* (*LPA1*) regulates both tiller angle and leaf angle in rice by controlling the adaxial growth of tiller node and lamina joint¹⁷. Rice *PROG1* encoding a putative finger transcription factor with C-terminal EAT-like repression domain also regulates tiller angle¹⁸. *ZmTAC1* in maize, the orthologous of rice *TAC1*, has

Oil Crops Research Institute of Chinese Academy of Agricultural Sciences/Key Laboratory for Biological Sciences and Genetic Improvement of Oil Crops, Ministry of Agriculture, No. 2 Xudong 2nd Road, Wuhan 430062, P.R. China. *These authors contributed equally to this work. Correspondence and requests for materials should be addressed to Q.H. (email: huqiong01@caas.cn)

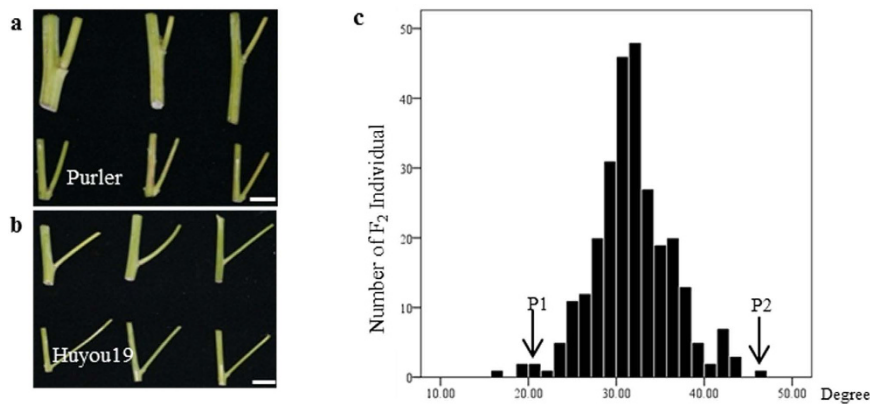


Figure 1. Phenotypes of Huyou19 and Purler with different branch angle and the frequency distribution of branch angle in F₂ population. (a) Purler (P₁); (b) Huyou 19 (P₂); Upper row: Angle of the lowest branch, lower row: Angle of the top branch. Bar = 2 cm. (c) Frequency distribution of branch angle of 277 individuals in F₂ population.

been demonstrated to be a major quantitative trait locus determining leaf angle¹⁹. Quite a few homologs of genes regulating branch angle in monocots also function in dicots. *AtLAZY1* in *Arabidopsis* has been demonstrated to regulate branch angle²⁰. *TAC1* was identified as the candidate gene for branch angle in peach, a dicot tree species²¹.

Auxin or polar auxin transports (PAT) were proven to be involved in the gravitropism and thereby regulating tiller angle in rice. Increasing the level of a polar auxin transporter OsPIN2 resulted in enlarged tiller angle²². The amount of PAT was greatly enhanced in *lazy* mutant and thus the endogenous IAA distribution in shoot was changed, leading to increased tiller angle^{15,23}. Recently, strigolactone (SL) biosynthetic or signaling mutants were identified to rescue the spreading phenotype of *lazy1*, suggesting that SLs can inhibit auxin biosynthesis and attenuate rice shoot gravitropism¹⁴. Potato plants overexpressing *AtYUCCA6* displayed smaller angle between petiole and stem and other high-auxin phenotypes, such as increased height, erect stature and longevity²⁴. *YUCCA* has long been revealed to be involved in the tryptamine (TAM) pathway, which is one of the four tryptophan-dependent auxin synthesis pathways²⁵. Recently, a two-step pathway of IAA biosynthesis in *Arabidopsis* from tryptophan was demonstrated^{26–29}. *YUCCAs* encode flavin monooxygenases which convert indole-3-pyruvic acid (IPA) to IAA in the second step of the two-step pathway of IAA biosynthesis²⁵. Overexpression of *YUCCAs* in *Arabidopsis* or rice resulted in high level of free IAA and therefore generated development defects associated with IAA accumulation^{30–32}. *YUCCA* orthologous in other species also appeared to function in auxin synthesis based on their effects on plant development^{32–34}. Similar to *AtYUCCA6*, other *YUCCA* orthologous involved in auxin synthesis may also play a role in the regulation of branch angle.

QTL mapping for genetic dissection of quantitative traits is useful for map-based cloning of related genes and marker-assist selection in plant breeding. However, the identification of polymorphic markers and genotyping of individuals from large segregation population is labor and cost consuming³⁵. The rapid development of high throughput sequencing methods has helped quick identification of polymorphic markers and quantitative trait locus (QTL) by genotyping³⁵. Bulked-segregant analysis (BSA) was widely used to rapidly identify markers linked to target genes or QTL by genotyping only two bulked DNA samples composed two opposite extremes of the interested trait in a segregating progeny³⁶. Several QTL were rapidly identified by the combination of whole-genome re-sequencing with BSA, which was also referred as QTL-seq^{37–41}. Recently, more QTL and candidate genes for agronomic traits were identified by QTL-seq, verifying the effectiveness of this approach^{42–45}.

Compared with the remarkable progress in the above mentioned plant species, study on branch angle in *Brassica napus* was just on the threshold. Significant negative genetic correlations between branch angle and yield per plant were observed⁴⁶. Twenty-five QTLs significantly associated with branch angle were identified after performing genome wide association study (GWAS) in a diversity panel⁴⁷. Branch angle is as crucial for the establishment of ideal plant architecture and yield improvement in *B. napus* as in other crops. Branch angle was significantly decreased with the increasing of row spacing under higher plant densities⁴⁸. Alteration of branch angle was considered to be well-suited for efficient light interception and easy operation of combine harvesting under higher plant density⁴⁸. In this paper, we conducted whole genome sequencing of two DNA bulks from plants with extreme branch angle selected from an F₂ population. Genome-wide SNP analysis allowed the detection of a genomic region harboring the major branch angle QTL and candidate genes were selected. Taken the advantage of conventional QTL analysis, expression pattern and phytohormones determination, we provided evidence that one gene which is the homolog of *AtYUCCA6* encoding flavin monooxygenase, located at chromosome A06 is a candidate gene for branch angle in *B. napus*.

Results

Inheritance of branch angle in *B. napus*. *B. napus* lines Huyou19 and Purler, harboring big and small branch angle respectively (Fig. 1a), were used to construct a segregation population. The average branch angle of Huyou19 (P₂) was approximately 32 degrees larger than that of Purler (P₁). The branch angle in F₂ population

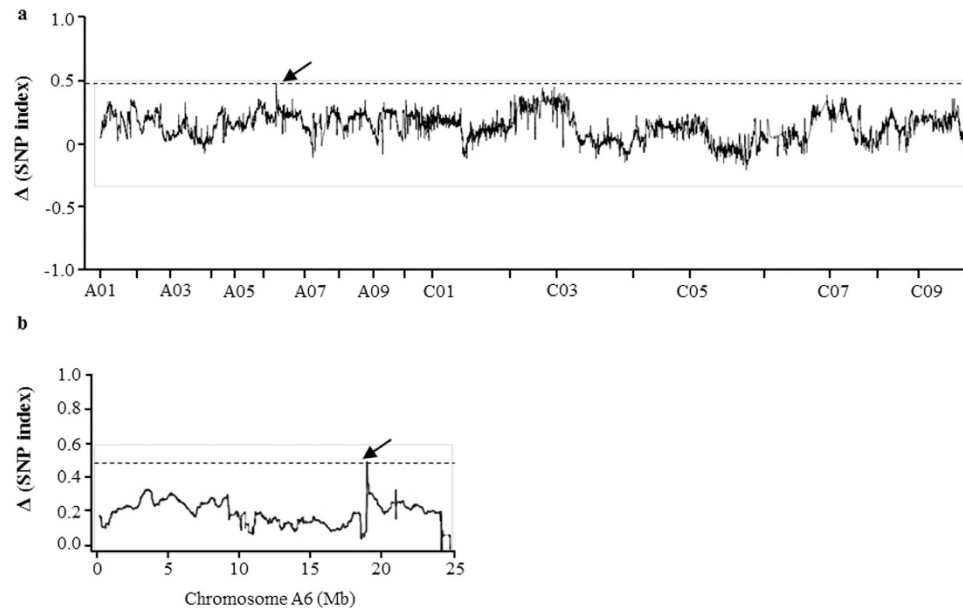


Figure 2. Δ SNP-index graphs from QTL-seq analysis. (a) X-axis represents the position of seven chromosomes and Y-axis represents the Δ SNP-index. SNP-index was calculated based on 1 Mb interval with a 5 kb sliding window. The Δ (SNP-index) graph was plotted with statistical confidence intervals under the null hypothesis of no QTL ($P < 0.05$). (b) One candidate QTL regions was identified in *B. napus* chromosome A06 (17.74–18.32 Mb interval) with the criteria that the SNP index in Big-pool was near 1, SNP-index in Small-pool was near 0 and the Δ (SNP-index) was above the confidence value ($P < 0.05$).

including 277 randomly selected individuals displayed continuous variation, but not a complete normal distribution, showing a skewed distribution with a skewness of 0.086 (Fig. 1b). This result suggested that the branch angle trait in *B. napus* was quantitatively inherited. Genetic analysis by the mixed major gene plus polygene inheritance model using six generations (P_1 , P_2 , F_1 , F_2 , BCP_1 and BCP_2) showed that branch angle in *B. napus* was controlled by a pair of major gene with additive-dominant effects plus polygenes with additive-dominance-epistasis effects (unpublished data).

Candidate QTL for branch angle identified by QTL-seq. Genomic DNA of the two parents (Huyou19 and Purler) and the two pools (B-pool and S-pool) was sequenced by Illumina HiSeq 2500 sequencer and resulted in 10.45 million clean reads. Most of the reads obtained were high quality, with $Q20 \geq 93.57$ and $Q30 \geq 88.25\%$ (Table S1). Ultimately, 289,333,224 and 294,048,030 reads from the two DNA pools were generated (Table S2). In total, 2,171,317 SNPs were identified between two parents. Short reads of all the samples were aligned to the *B. napus* reference genome⁴⁹. The SNP index of the two DNA pools was calculated for each identified SNP. SNP-index graph of B-pool and S-pool was shown in Supplementary Figure 1. Δ (SNP-index) was calculated and plotted to the genome position by combining the information of SNP-index in B-pool and S-pool (Fig. 2a). According to the null hypothesis, we chose peak regions above the threshold value (threshold value = 0.487) as the candidate region harboring major QTL for target trait (Fig. 2a). With 95% significance level, a genomic region (A06: 17.74–18.32 Mb) was found to hold the Δ (SNP-index) value above the threshold and was referred as the target region for branch angle (Fig. 2b).

Validation of identified QTL by Indel markers. To verify the QTL predicted from QTL-seq, traditional QTL mapping was performed in the F_2 population with 277 individual plants. In total, 658,715 Indel markers distributed at different genomic regions were detected according to high-throughput sequencing data (Table S3). Thirteen polymorphic markers located in the candidate region were used to genotyping 277 F_2 plants and the data were used for linkage analysis. One major QTL located within about 82 kb physical distance on A06 was detected by Inclusive Composite Interval Mapping (ICIM) analysis for branch angle. This QTL with a LOD value of 11 accounts for 17.17% of phenotypic variance (Fig. 3). This result was consistent with that obtained from Δ (SNP-index) analysis of QTL-seq, supporting that a QTL locus for branch angle is located in the genome interval of A06, 17.74–18.32 Mb.

Identification of candidate genes for branch angle. Totally 82 genes were predicted in the A06: 17.74–18.32 Mb region delimited by two Indel markers A06Indel76 and A06Indel79. Three genes (*BnaA06g32200D*, *BnaA06g32210D* and *BnaA06g39380D*) were identified after filtration. *BnaA06g39380D* is a homolog of Arabidopsis *YUCCA6* which is involved in *de novo* auxin biosynthesis pathway²⁵ and leaf angle modulation²⁴. We nominated the *BnaA06g39380D* gene as “*BnaA.YUCCA6.a*” (Gene accession number: KX35886) based on the standard nomenclature of Østergaard and King⁵⁰. To verify whether *BnaA06g39380D* is the candidate gene, genomic and complementary DNA (cDNA) sequences of this gene were cloned and sequenced from

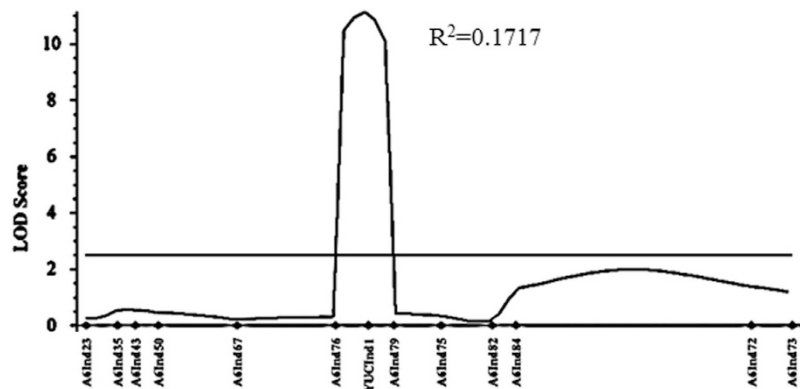


Figure 3. Genetic validation of branch angle QTL *ba1* in *Brassica napus* chromosome A06 using an F_2 population. Linkage analysis confirmed the branch angle QTL with flanking markers A06Indel76 to A06Indel79. Candidate gene *BnaA06g39380D* was located at the peak of QTL interval. The location of *ba1* was generated using inclusive composite interval mapping (ICIM). The x-axis indicates the genetic distance of Indel markers. The y-axis indicates the LOD score of QTL. R^2 is the phenotypic variance contributed by QTL *ba1*.

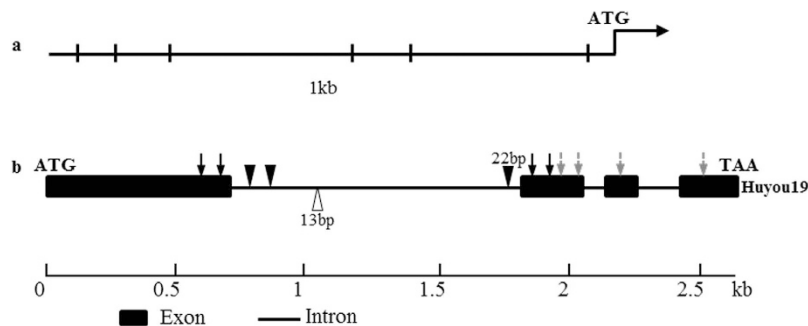


Figure 4. Structure and sequence variation of *BnaYUCCA6* between Huyou19 and Purler. (a) Comparison of promoter sequence of *BnaYUCCA6* between Huyou19 and Purler. Vertical bar represents nucleotide variation in promoter region; (b) Gene structure and mutation type of *BnaYUCCA6* in Huyou19 compared with Purler. Black and gray arrows represent non-synonymous and synonymous mutation in coding region, respectively. Inverted and positive triangles represent nucleotide insertion and deletion in the first intron, respectively. Size of exons and introns can be estimated using the scale bar at bottom.

the two parents. Sequence comparison between the alleles of two parents showed that there are nine SNPs in the two exons both on DNA and cDNA levels (Fig. 4). Four amino acid variations were detected after aligning the predicted protein sequences of *BnaA06g39380D* in the two parent lines. Meanwhile, one 22-bp insertion in the first intron of Huyou19 allele was detected and a gene specific Indel marker (YUC6Indel1) was developed. This marker YUC6Indel1 was mapped right at the LOD curve peak for branch angle QTL (Fig. 3).

Expression patterns of *YUCCA6* in two parental lines at different tissues were investigated to analyze whether the expression level of *YUCCA6* is associated with the variance of branch angle. The expression level of *YUCCA6* showed different among tissues. However, in all the three tissues examined, significantly higher *YUCCA6* expression was observed in the small branch angle line Purler than in the big branch angle line Huyou19 (Fig. 5). For other two identified genes, only one SNP variation has been detected in promoter region of gene *BnaA06g32200D*, homolog of which encodes hydrolases in *Arabidopsis*. We detected only one non-synonymous mutation in coding region of gene *BnaA06g32210D* which was predicted to encode a plant UBX-domain contained protein. None evidence showed that the function of these two genes is associated with plant hormone signaling or branch angle regulation. Meanwhile, no different expression of these two genes has been detected between two parents in three tissue samples (Fig. 5).

Previous results have emphasized the pivotal role of *YUCCA* in auxin biosynthesis. In order to investigate if IAA as a major auxin component is related to branch angle phenotype, IAA was measured in the two parental lines of different tissues. The result showed that IAA content was significantly increased in Purler compared with that in Huyou19 in leaf, axillary shoot and stem tissues (Fig. 6). All these results support that *YUCCA6* is a candidate gene for major QTL controlling branch angle in *B. napus*, though further genetic transformation assay needs to be performed for functional validation of the gene.

Phylogenetic analysis of *BnaYUCCA6*. Eleven and fourteen *YUCCA* genes from *Arabidopsis* and rice, which are model plants for monocot and dicot species respectively, were extracted from the public database (<http://www.dtd.nlm.nih.gov/>). Five homologs were identified in the *B. napus* genome by using *AtYUCCA6*

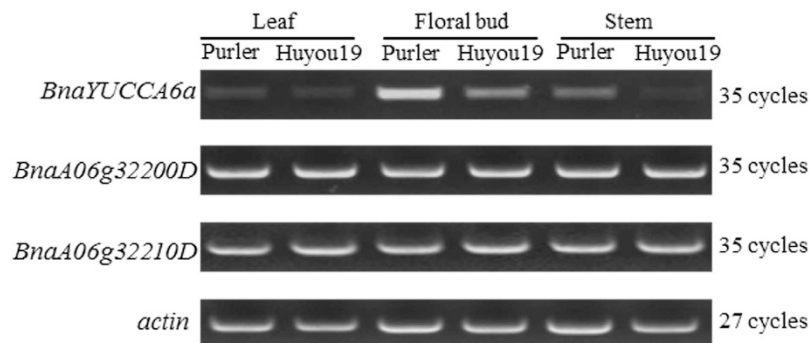


Figure 5. Transcript level of *BnaYUCCA6* in Huyou19 and Purler. The expression level of *BnaYUCCA6*, *BnaA06g32200D* and *BnaA06g32210D* was conducted by RT-PCR using gene specific primers. *Actin* was used as an internal reference gene with 27 cycles.

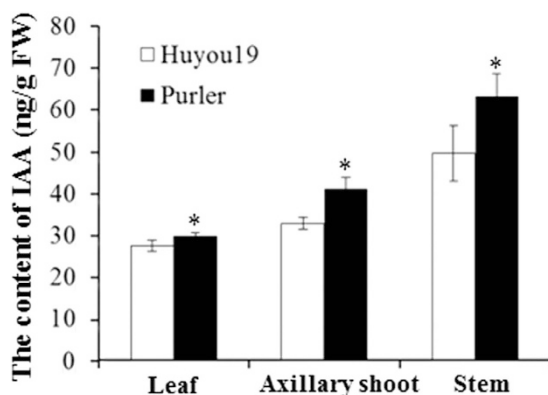


Figure 6. IAA of three tissue samples in Huyou19 and Purler. The data represent three independent experiments. Asterisks indicate a significant difference was detected between Huyou19 and Purler in the same tissue sample at $*P < 0.05$.

as query against the “pseudomolecules” representative of the *B. napus* genome (version 4)⁴⁹. Two AtYUCCA6 homologs were obtained from *Brassica rapa* and *Brassica oleracea* genome respectively. Alignment of amino acid sequences of YUC6-like genes from *B. napus*, *B. rapa* and *B. oleracea* showed that the motifs of YUCCA6 protein were highly conserved, all containing FAD-binding domain, FMO-identifying domain and NADP-binding domain (Fig. 7). A total of 32 YUCCA proteins were used for the construction of an unrooted phylogenetic tree. Phylogenetic analysis showed that the homologs of AtYUCCA6 from Brassica species were clustered in one individual group, indicating the conservation of YUCCA proteins among Brassica species during evolutionary process. Apart from very high similarity to the counterparts from *B. napus*, YUCCA6 also showed in general a closer relationship with its orthologs in *B. rapa* and *B. oleracea* (Fig. 8). YUCCA6 proteins from dicots *B. napus*, *B. rapa*, *B. oleracea* and *Arabidopsis thaliana* were clustered in a big group, which also implies their functional consistence.

Discussion

Methods based on molecular marker development have made tremendous progress in genotyping and QTL mapping. For genetic map construction and genetic dissection of quantitative traits, QTL mapping using traditional markers is considered to be most reliable. However, traditional QTL mapping is usually conducted by genotyping a large number of individuals in a primary population and then fine mapping candidate genes in advanced populations, which is very time-consuming and painstaking³⁵. QTL-seq integrated the advantages of BSA and high-throughput whole genome re-sequencing, has been proven to be an efficient and quick method to ascertain the genomic regions harbor QTL for quantitative traits. Previous results showed that QTL-seq can be applied in RIL or F_2 populations to identify QTL for different agronomic traits undergone artificial or natural selective sweeps³⁷. Since the first article published in yeast³⁶, many QTL or candidate genes have been identified in different plant species by QTL-seq^{38–44}. Previous results by genome wide association study (GWAS) showed that there are twenty-five QTL associated with branch angle in a diversity panel⁴⁶. In this study, we identified one QTL for branch angle in *B. napus* by QTL-seq using an F_2 population. This QTL was verified by traditional mapping approach and a candidate gene responsible for branch angle was predicted. The whole procedure took only 2.5 years including 1.5 years for F_2 population construction. Although high-throughput sequencing is expensive now, it is still worthwhile since a lot of time and labor input can be significantly reduced. For a plant species which has a reference whole genome sequence such as oilseed rape, QTL-seq is a highly effective approach for identify major QTL or candidate genes for quantitative traits.

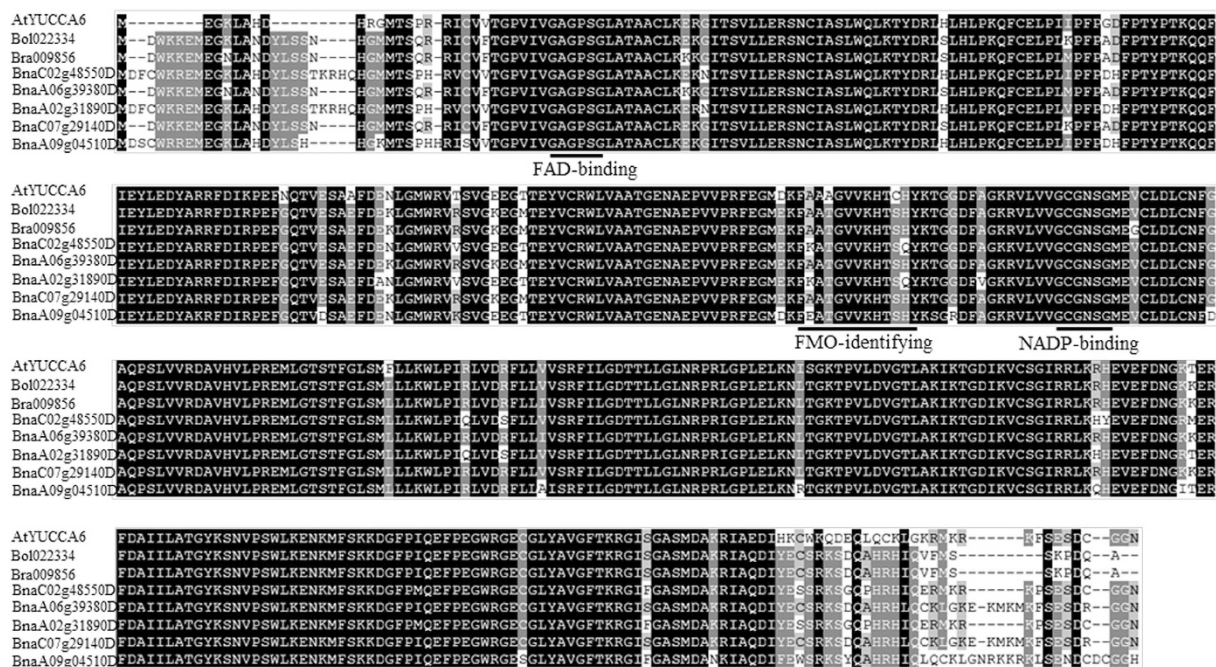


Figure 7. Comparison of amino acid sequences of *AtYUCCA6* and *YUCCA6*-like genes from *Brassica napus*, *Brassica rapa* and *Brassica oleracea*. The sequences were aligned by ClustalW and edited by Gendoc. The conserved motifs of YUCCA proteins are shown at the appropriate location.

QTL-seq has rarely been applied in *Brassica* species⁵¹. Seventy SNPs associated with pod shatter resistance was identified by using similar approach. In their study, a major QTL *psr1* for pod shatter resistance was mapped by sequencing reduced representation libraries of two bulked samples of plants with contrasting pod shatter resistance from an F₂ population using restriction digests and size selection⁵¹. This QTL was confirmed by traditional mapping with the F₂ population and genome-wide association studies with diverse *B. napus* germplasm⁵². However, none candidate gene was predicted even though the QTL was confined within a 396 kb genomic region on A09 chromosome of *B. rapa* at that time. After two years, *SHP1* was predicted to be a candidate gene of the A09 locus using the whole genome sequence of *B. rapa* by another group⁵². Limiting factors for the failure of gene prediction in the previous study⁵¹ include lacking of *B. napus* reference genome sequence and re-sequencing information of parental lines at that time. Since there are usually frequent rearrangements of genome fragments between the A genomes from *B. napus* and *B. rapa*^{53,54}, as well as among genomes from different varieties among *B. napus* lines^{55,56}, genomic sequence information of parental lines is of great importance for candidate gene prediction within the targeted QTL region. Our study taking the advantage of re-sequencing the parental lines, made prediction of candidate genes easier by sequence comparison of genes within the 580 kb QTL genomic region.

As a quantitative trait, branch angle is certainly not only controlled by one locus. More loci could be detected when the threshold value of Δ (SNP-index) is decreased. In order to include as many loci as possible, 30 individuals with extreme phenotype from F₂ population were selected to combine the DNA pool, which contained plants with relatively wide range of branch angle values. Higher percentage of F₂ individuals included in the extreme bulks will increase the power to detect causal QTL despite allele frequency difference can be relatively smaller between bulks^{40,57}. Nevertheless, the locus detected in this study with the highest Δ (SNP-index) value has the highest chance to be actually associated with the branch angle trait.

YUCCA6, an *AtYUCCA6* homologous gene located at the A06 *ba1* QTL region was identified as a candidate gene for branch angle based on gene sequence variation, physical mapping, functional prediction by phylogenetic analysis as well as differential expression. YUCCA genes encode flavin monooxygenases and function in the second step in *de novo* auxin biosynthesis pathway²². Seedlings of the *yuc1yuc2yuc4yuc6* mutant accumulate more IPA, suggesting the YUCCA functioned in the step of IPA to IAA conversion^{26,29}. Plants overexpressed *Arabidopsis AtYUCCA6* displayed high-auxin phenotypes in *Arabidopsis*, potato and tobacco, including reduced angle between petiole and stem²⁴. These results suggest that *AtYUCCA6* was involved in auxin biosynthesis modulating leaf angle as well as other auxin-related phenotypes. YUCCA proteins contain two conserved motifs for FAD and NADPH binding respectively. Mutations of the two binding sites completely abolished YUCCA function in *Arabidopsis*⁵⁸. Sequence alignment showed that no amino acid variation was detected at the conserved motifs of YUCCA6a in the two parent lines, suggesting that the function of YUCCA6 alleles in the two parent lines may be no different. However, six SNP variations were detected after comparison of promoter sequences of YUCCA6 in the two parent lines. One SNP occurred in the *cis*-element bound by ARR1 (*Arabidopsis* response regulator) which functions as cytokinin receptor genes. Complex cross-talk between auxin and cytokinin and integration of hormone signaling are required for differentiation and maintenance of plant meristems as well as other developmental process⁵⁹. Previous results showed that ARR1 activated the gene *SHY2/IAA3* (*SHY2*) which

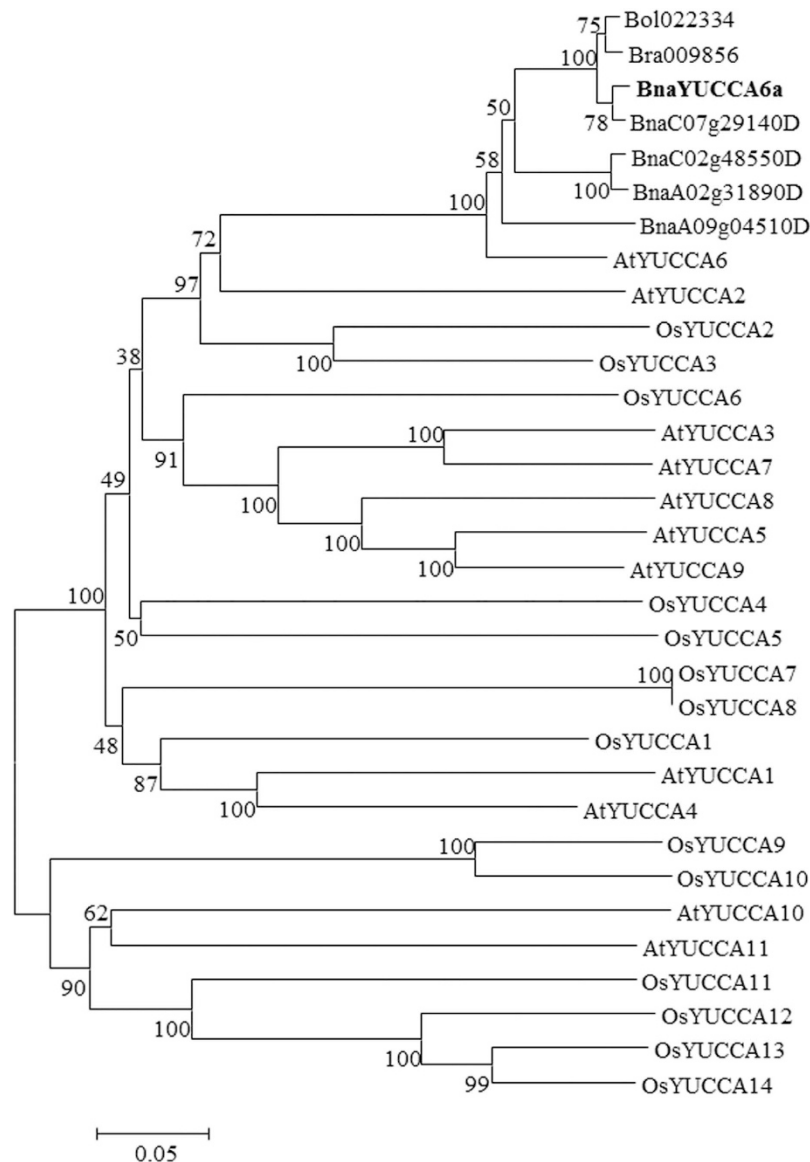


Figure 8. Phylogenetic analysis of YUCCA proteins. The YUCCA proteins from *Arabidopsis* (AtYUCCA), rice (OsYUCCA) and YUCCA6 protein in *B. napus* were aligned using ClustalW. The phylogenetic tree was constructed using the neighbor-joining algorithm with 1000 replication. Bar indicates 0.05 aa substitution per residue.

functions as a repressor of auxin signaling and negatively regulates polar auxin transport⁶⁰. Therefore, mutation within the cis-element of Purler promoter may result in loss of the suppression activity by cytokinin response regulator ARR1. Expression of *YUCCA6* may be influenced due to these SNPs in the promoter region and thus impact the auxin *de novo* synthesis, giving rise to the higher expression of *YUCCA6* and IAA content in Purler, leading to increased branch angle ultimately. All these analysis enables us to postulate that *YUCCA6* is the candidate gene for branch angle regulation. Studies with transgenic plants overexpressing *YUCCA6* in small branch angle lines will be needed for functional validation of this gene. Further study focus on the molecular characterization of *YUCCA6* may not only provide genetic resource to improve the yield of *B. napus* but also shed light on the role of auxin biosynthesis in branch angle regulation.

Methods

Plant materials and phenotyping for branch angle. One method for precisely measuring branch angle in *B. napus* was established previously⁴⁶. At adult stage, the first and the last branch node of each plant was cut and packed in one envelop to dry. Picture of the branch node was taken by a digital camera (DSLR-A350, SONY, Japan) on a flat platform and analysed using AutoCAD software. The branch angle value of a plant was calculated as the average of branch angles from the first and the last branch node. Purler and Huyou19 which harbor small and big branch angle, respectively, were selected as the parental lines to develop F₂ segregation population. A cross was made between Purler (female parent, P₁) and Huyou19 (pollen donor, P₂) to create F₁ plants.

F₂ population was generated by self-pollination of F₁ plants. All plant materials were grown in the field of Oil Crops Research Institute of the Chinese Academy of Agricultural Sciences (OCRI-CAAS), Wuhan, China. Equal amount of DNA from thirty of 277 F₂ plants with the smallest branch angle (19.26–27.15 degrees) was mixed to form the small branch angle bulk (S-pool), and that from another thirty plants with the biggest branch angle (42.77–57.88 degrees) was mixed to form the big branch angle bulk (B-pool).

Generation and analysis of NGS data. Sequence data of two bulks and two parents were generated by Illumina HiSeq 2500 and analyzed by Novogene (No. 38, Xueqing road, Haidian district, Beijing, <http://www.novogene.com>). In order to ensure the reads being reliable without artificial bias, such as low quality paired reads, which mainly resulted from base-calling duplicates and adapter contamination, raw data (raw reads) were firstly processed through a series of quality control (QC) procedures. BWA (Burrows-Wheeler Aligner) was used to align the clean reads from two DNA bulks against the reference genome of *B. napus*^{50,61,62}. Alignment files were converted to BAM files using SAMtools software⁶³. In addition, potential PCR duplications were removed using SAM tools command “rmdup”. If multiple read pairs have identical mapping site, only the pair with the highest mapping quality was retained.

SNPs or Indels were detected using the VariantFiltration parameter and annotated according to GFF3 files aligned with the reference genome by an efficient software tool ANNOVAR⁶⁴. Homozygous SNPs between the two parents were extracted from vcf files. The genotype of one parent was used as the reference to calculate the number of reads of this parent's genotype in the individuals of the offspring pools. The ratio of reads harboring SNP which is different from the reference sequence was calculated as the SNP index of the base site. Positions with SNP-index less than 0.3 were filtered out, as which may due to sequencing or alignment errors. Sliding window methods were used to present SNP index of the whole genome. The SNP index for each window was calculated as the average of all SNP index in that area of the genome. As usual, we defined window size as 1 Mb and step size as 10Kb according to the default setting. The difference of SNP index of the two pools was calculated as Δ (SNP index). Computer simulation was carried out to generate the confidence intervals of the SNP-index value under null hypothesis with no QTL, and the confidence intervals of Δ (SNP-index) were defined to be 95% as described previously⁴⁰.

QTL analysis by Indel marker. The QTL identified from QTL-seq were confirmed by conventional genetic linkage analysis. Reads from both parents were aligned to the *B. napus* reference genome (<http://www.genoscope.cns.fr/brassicapapus/data>) with BWA/SAMtools software. Gene specific Indel markers were exploited by comparison of candidate gene sequences between the two parents and then primers were designed by Primer Premier 5 based on sequence differences. PCR reaction was conducted using the following program: 5 min at 95 °C, 14 cycles of 30 s at 95 °C, 40 s at 64 °C and 1 min at 72 °C, then 24 cycles of 30 s at 95 °C, 40 s at 50 °C and 1 min at 72 °C. Individuals of the F₂ population were genotyped using Indel markers exhibited clearly polymorphic between parental lines within the candidate region. Linkage analysis and QTL mapping was operated with the inclusive composite interval mapping (ICIM) procedure^{65,66}. The ICIM of QTL was done by using QTL IciMapping software (<http://www.isbreeding.net>) and BIP (QTL mapping in bi-parent population) functionality. ICIM-ADD method was used to map. The largest *P* value for entering variables in stepwise regression of phenotype on marker variables was 0.001. The step size was 1 cM. A LOD score threshold of 2.5 was used to declare the existence of a QTL.

Candidate gene analysis. Based on the sequencing data of parental lines, sequences of the predicted genes within the A06 17.74–18.32 Mb QTL region were compared between the parents. SNP sites with significantly different SNP-index (with SNP-index ≥ 0.8 in B-pool and ≤ 0.2 in S-pool) were selected as polymorphic marker loci. According to the annotation result of ANNOVAR, genes with SNPs causing stop gain or loss and non-synonymous mutation in their corresponding alleles were selected as candidate genes. Meanwhile, genes with SNPs in the promoter region prior to start codon ATG (≤ 1 kb) in their corresponding alleles were also selected as candidate genes.

Expression analysis by semi-quantitative RT-PCR. We investigated the expression pattern of the candidate genes. Samples of leaf, stem and floral bud were collected from five different individuals of Purler and Huyou19 at bolting stage and pooled with equal amount of tissue from each plant. Total RNAs for all the samples were extracted with Trizol Reagent (Invitrogen, America). Reverse transcription was performed according to the instruction of FastQuant RT Kit (Tiangen, China). RT-PCR was performed as described previously using the primers listed in Table S5. The expression level of actin gene in *B. napus* was used to standardize the RNA sample for each RT-PCR. The reaction was conducted using following program: 5 min at 95 °C, 35 cycles of 30 s at 95 °C, 40 s at 56 °C and 1 min at 72 °C.

IAA Quantification. Three tissue samples: leaf, stem and axillary shoot were used for IAA quantification. Samples were prepared and mixtures of compounds were separated by HPLC (Agilent 1200) and analyzed using a hybrid triple quadrupole/linear ion trap mass spectrometer (ABI 4000 Q-Trap, Applied Biosystems, Foster City, CA, USA). IAA was quantified according to the method described previously⁶⁷.

Phylogenetic analysis of YUCCA genes. Blastp was performed against *B. napus* genome data using AtYUCCA6 protein sequence as query. YUCCA family members from *Arabidopsis* were downloaded from TAIR (<http://www.Arabidopsis.org/>). Rice YUCCA genes were downloaded from rice genome project (<http://rice.plantbiology.msu.edu/>). Multiple sequence alignment of YUCCA protein sequence from *Oryza sativa*, *Arabidopsis thaliana* and *B. napus* was performed using ClustalX2.0 with default parameters. Sequence alignment was further edited by Gendoc software. Phylogenetic trees were constructed by MEGA6.0 software using the neighbor-joining (NJ) method with 1000 bootstrap replications.

References

1. Kebrom, T. H. & Brutnell, T. P. The molecular analysis of the shade avoidance syndrome in the grasses has begun. *J. Exp. Bot.* **58**, 3079–3089 (2007).
2. Nik, M. M., Babaeian, M., Tavassoli, A. & Asgharzade, A. Effect of plant density on yield and yield components of corn hybrids (*Zea mays*). *Sci. Res. Essays* **6**, 4821–4825 (2011).
3. Mansfield, B. D. & Mumm, R. H. Survey of plant density tolerance in US maize germplasm. *Crop Sci.* **54**, 157–173 (2014).
4. Duvíček, D. N. Genetic progress in yield of United States maize (*Zea mays* L.). *Maydica* **50**, 193–202 (2005).
5. Reinhardt, D. & Kuhlemeier, C. Plant architecture. *EMBO Rep.* **3**, 846–851 (2002).
6. Wang, Y. H. & Li, J. Y. Genes controlling plant architecture. *Curr. Opin. Biotechnol.* **17**, 123–129 (2006).
7. Wang, Y. H. & Li, J. Y. Branching in rice. *Curr. Opin. Plant Biol.* **14**, 94–99 (2011).
8. Zhao, H. *et al.* Natural variation and genetic analysis of the tiller angle gene *MsTAC1* in *Miscanthus sinensis*. *Planta* **240**, 161–175 (2014).
9. Truong, S. K. *et al.* Harnessing Genetic Variation in Leaf Angle to Increase Productivity of *Sorghum bicolor*. *Genetics* **201**, 1229–1238 (2015).
10. Tian, F. *et al.* Genome-wide association study of leaf architecture in the maize nested association mapping population. *Nature Genetics* **43**, 159–162 (2011).
11. Liang, W. H., Shang, F., Lin, Q. T., Lou, C. & Zhang, J. Tillering and panicle branching genes in rice. *Gene* **537**, 1–5 (2014).
12. Sang, D. J. *et al.* Strigolactones regulate rice tiller angle by attenuating shoot gravitropism through inhibiting auxin biosynthesis. *Proc. Natl. Acad. Sci. USA* **111**, 11199–11204 (2014).
13. Roychoudhry, S. *et al.* Auxin controls gravitropic setpoint angle in higher plant lateral branches. *Curr Biol* **23**, 1497–1504 (2013).
14. Cui, D. *et al.* The arabidopsis *IDD14*, *IDD15*, and *IDD16* cooperatively regulate lateral organ morphogenesis and gravitropism by promoting auxin biosynthesis and transport. *PLoS Genet* **9**, e1003759 (2013).
15. Li, P. J. *et al.* *LAZY1* controls rice shoot gravitropism through regulating polar auxin transport. *Cell Res.* **17**, 402–410 (2007).
16. Yu, B. S. *et al.* *TAC1*, a major quantitative trait locus controlling tiller angle in rice. *Plant J.* **52**, 891–898 (2007).
17. Wu, X. R., Tang, D., Li, M., Wang, K. J. & Cheng, Z. K. Loose plant architecture1, an INDETERMINATE DOMAIN protein involved in shoot gravitropism, regulates plant architecture in rice. *Plant Physiol.* **161**, 317–329 (2013).
18. Tan, L. B. *et al.* Control of a key transition from prostrate to erect growth in rice domestication. *Nat. Genet* **40**, 1360–1364 (2008).
19. Ku, L. X. *et al.* Cloning and characterization of a putative *TAC1* ortholog associated with leaf angle in maize (*Zea mays* L.). *PLoS ONE* **6**, e20621 (2011).
20. Yoshihara, T., Spalding, E. P. & Iino, M. AtLAZY1 is a signaling component required for gravitropism of the *Arabidopsis thaliana* inflorescence. *Plant J.* **74**, 267–279 (2013).
21. Dardick, C. *et al.* PpeTAC1 promotes the horizontal growth of branches in peach trees and is a member of a functionally conserved gene family found in diverse plants species. *Plant J.* **75**, 618–630 (2013).
22. Chen, Y. N., Fan, X. R., Song, W. J., Zhang, Y. L. & Xu, G. H. Over-expression of *OsPIN2* leads to increased tiller numbers, angle and shorter plant height through suppression of *OsLAZY1*. *Plant Biotechnol. J.* **10**, 139–149 (2012).
23. Fu, X. D. & Zuo, J. R. PAT: waking up a lazy sleeping beauty. *Cell Res.* **17**, 402–410 (2007).
24. Kim, J. I. *et al.* Overexpression of Arabidopsis *YUCCA6* in potato results in high-auxin developmental phenotypes and enhanced resistance to water deficit. *Mol. Plant.* **6**, 337–349 (2013).
25. Zhao, Y. D. Auxin biosynthesis: a simple two-step pathway converts tryptophan to indole-3-acetic acid in plants. *Mol. Plant* **5**, 334–338 (2012).
26. Mashiguchi, K. *et al.* The main auxin biosynthesis pathway in Arabidopsis. *Proc. Natl. Acad. Sci. USA* **108**, 18512–18517 (2011).
27. Ross, J. J. *et al.* Reassessing the role of YUCCAs in auxin biosynthesis. *Plant Signal. Behav.* **6**, 437–439 (2011).
28. Stepanova, A. N. *et al.* The Arabidopsis *YUCCA1* flavin monooxygenase functions in the indole-3-pyruvic acid branch of auxin biosynthesis. *Plant Cell* **23**, 3961–3973 (2011).
29. Won, C. *et al.* Conversion of tryptophan to indole-3-acetic acid by Tryptophan aminotransferases of *Arabidopsis* and YUCCAs in *Arabidopsis*. *Proc. Natl. Acad. Sci. USA* **108**, 18518–18523 (2011).
30. Zhao, Y. D. *et al.* A role for flavin monooxygenase-like enzymes in auxin biosynthesis. *Science* **291**, 306–309 (2001).
31. Kim, J. I. *et al.* *yucca6*, a dominant mutation in Arabidopsis, affects auxin accumulation and auxin-related phenotypes. *Plant Physiol.* **145**, 722–735 (2007).
32. Yamamoto, Y., Kamiya, N., Morinaka, Y., Matsuoka, M. & Sazuka, T. Auxin biosynthesis by the *YUCCA* genes in rice. *Plant Physiol.* **143**, 1362–1371 (2007).
33. Tobeha-Santamaria, R. *et al.* FLOOZY of petunia is a flavin mono-oxygenase-like protein required for the specification of leaf and flower architecture. *Genes Dev.* **16**, 753–763 (2002).
34. Expósito-Rodríguez, M., Borges, A. A., Borges-Pérez, A., Hernández, M. & Pérez, J. A. Cloning and biochemical characterization of *ToFZY*, a tomato gene encoding a flavin monooxygenase involved in a tryptophan-dependent auxin biosynthesis pathway. *J. Plant Growth Regul.* **26**, 329–340 (2007).
35. Salvi, S. & Tuberosa, R. To clone or not to clone plant QTLs: present and future challenges. *Trends Plant Sci.* **10**, 297–304 (2005).
36. Michelmore, R. W., Paran, I. & Kesseli, R. V. Identification of markers linked to disease-resistance genes by bulked segregant analysis: a rapid method to detect markers in specific genomic regions by using segregating populations. *Proc. Natl. Acad. Sci. USA* **88**, 9828–9832 (1991).
37. Wenger, J. W., Schwartz, K. & Sherlock, G. Bulk segregant analysis by high-throughput sequencing reveals a novel xylose utilization gene from *Saccharomyces cerevisiae*. *PLoS Genet.* **6**, e1000942 (2010).
38. Abe, A. *et al.* Genome sequencing reveals agronomically important loci in rice using MutMap. *Nat. Biotechnol.* **30**, 174–178 (2012).
39. Trick, M. *et al.* Combining SNP discovery from next-generation sequencing data with bulked segregant analysis (BSA) to fine-map genes in polyploid wheat. *BMC Plant Biol.* **12**, 14 (2012).
40. Takagi, H. *et al.* QTL-seq: rapid mapping of quantitative trait loci in rice by whole genome resequencing of DNA from two bulked populations. *Plant J.* **74**, 174–183 (2013).
41. Yang, Z. M. *et al.* Mapping of quantitative trait loci underlying cold tolerance in rice seedlings via high-throughput sequencing of pooled extremes. *PLoS ONE* **8**, e68433 (2013).
42. Lu, H. F. *et al.* QTL-seq identifies an early flowering QTL located near Flowering Locus T in cucumber. *Theor. Appl. Genet.* **127**, 1491–1499 (2014).
43. Qin, D. D. *et al.* Characterization and fine mapping of a novel barley Stage Green-Revertible Albino Gene (*HvSGRA*) by Bulk Segregant Analysis based on SSR assay and Specific Length Amplified Fragment Sequencing. *BMC Genomics* **16**, 838 (2015).
44. Xu, X. W. *et al.* QTL mapping of cucumber fruit flesh thickness by SLAF-seq. *Sci. Rep.* **5**, 15829 (2015).
45. Lu, H. *et al.* QTL-seq identifies an early flowering QTL located near Flowering Locus T in cucumber. *Theor. Appl. Genet.* **127**, 1491–1499 (2014).
46. Wang, J. S. *et al.* Study on the heredity of plant-type traits in compact rapeseed lines and the genetic correlation with yield traits. *Journal of Northwest Sci-Tech University of Agriculture and Forestry* **33**, 7–12 (2005).
47. Liu, J. *et al.* Characterizing Variation of Branch Angle and Genome-Wide Association Mapping in Rapeseed (*Brassica napus* L.). *Front Plant Sci.* **7**, 21 (2016).

48. Kuai, J. *et al.* The yield of mechanically harvested rapeseed (*Brassica napus* L.) can be increased by optimum plant density and row spacing. *Sci Rep.* **5**, 18835 (2015).
49. Chalhoub, B. *et al.* Early allopolyploid evolution in the post-Neolithic *Brassica napus* oilseed genome. *Science* **345**, 950–953 (2014).
50. Østergaard, L. & King, G. J. Standardized gene nomenclature for the Brassica genus. *Plant Methods* **4**, 10 (2008).
51. Hu, Z. Y. *et al.* Discovery of pod shatter-resistant associated SNPs by deep sequencing of a representative library followed by bulk segregant analysis in rapeseed. *PLoS ONE* **7**, e34253 (2012).
52. Raman, H. *et al.* Genome-wide delineation of natural variation for pod shatter resistance in *Brassica napus*. *PLoS ONE* **9**, e101673 (2014).
53. Xu, J. S. *et al.* Construction of an integrated genetic linkage map for the A genome of *Brassica napus* using SSR markers derived from sequenced BACs in *B. rapa*. *BMC Genomics* **11**, 594 (2010).
54. Li, N., Shi, J. Q., Wang, X. F., Liu, G. H. & Wang, H. Z. A combined linkage and regional association mapping validation and fine mapping of two major pleiotropic QTLs for seed weight and silique length in rapeseed (*Brassica napus* L.). *BMC Plant Biol.* **14**, 114 (2014).
55. Udall, J. A. & Quijada, P. A. Osborn TC: Detection of chromosomal rearrangements derived from homologous recombination in four mapping populations of *Brassica napus* L. *Genetics* **169**, 967–979 (2005).
56. Qian, L. W., Qian, W. & Snowdon, R. J. Sub-genomic selection patterns as a signature of breeding in the allopolyploid *Brassica napus* genome. *BMC Genomics* **15**, 1–17 (2014).
57. Magwene, P. M. *et al.* The statistics of bulk segregant analysis using next generation sequencing. *PLoS Comput Biol.* **7**, e1002255 (2011).
58. Hou, X. H. *et al.* Allelic analyses of the Arabidopsis *YUC1* locus reveal residues and domains essential for the functions of YUC family of flavin monooxygenases. *J. Integr. Plant Biol.* **53**, 54–62 (2011).
59. Su, Y. H., Liu, Y. B. & Zhang, X. S. Auxin-cytokinin interaction regulates meristem development. *Mol. Plant* **4**, 616–625 (2011).
60. Ioio, D. R. *et al.* A genetic framework for the control of cell division and differentiation in the root meristem. *Science* **322**, 1380–1384 (2008).
61. Chalhoub, B. *et al.* Early allopolyploid evolution in the post-Neolithic *Brassica napus* oilseed genome. *Science* **345**, 950–953 (2014).
62. Li, H. & Durbin, R. Fast and accurate short read alignment with Burrows-Wheeler transform. *Bioinformatics* **25**, 1754–1760 (2009).
63. Li, H. *et al.* The sequence alignment/map format and SAMtools. *Bioinformatics*, **25**, 2078–2079 (2009).
64. Wang, K., Li, M. Y. & Hakonarson, H. ANNOVAR: functional annotation of genetic variants from high-throughput sequencing data. *Nucleic Acids Res.* **38**, e164 (2010).
65. Li, H. H., Ye, G. Y. & Wang, J. K. A modified algorithm for the improvement of composite interval mapping. *Genetics* **175**, 361–374 (2007).
66. Zhang, L. Y., Li, H. H., Li, Z. L. & Wang, J. K. Interactions between markers can be caused by the dominance effect of QTL. *Genetics* **180**, 1177–1190 (2008).
67. Li, Y. H. *et al.* Simultaneous analysis of multiple endogenous plant hormones in leaf tissue of oilseed rape by solid-phase extraction coupled with high-performance liquid chromatography-electrospray ionisation tandem mass spectrometry. *Phytochem. Anal.* **22**, 442–449 (2011).

Acknowledgements

This work was supported by the Science and technology innovation project of Chinese Academy of Agricultural Sciences (Group No. 118), the Earmarked Fund for China Agriculture Research System (CARS-13), the Hubei Agricultural Science and Technology Innovation Center and Hubei National Science Foundation (2014CFB156, 2015CFA103).

Author Contributions

H.W., H.C. and H.Q. designed research. J.L. and W.W. constructed the genetic population and measured branch angle. H.W. and D.M. performed QTL analysis. H.C. and M.H. performed RT-PCR and IAA determination. R.Z. and L.F. provided plant material and prepared RNA samples. H.W. and H.C. interpreted the data and wrote the paper. H.Q. supervised the whole study. All authors have read and approved the version of manuscript.

Additional Information

Supplementary information accompanies this paper at <http://www.nature.com/srep>

Competing financial interests: The authors declare no competing financial interests.

How to cite this article: Wang, H. *et al.* Identification of *BnaYUCCA6* as a candidate gene for branch angle in *Brassica napus* by QTL-seq. *Sci. Rep.* **6**, 38493; doi: 10.1038/srep38493 (2016).

Publisher's note: Springer Nature remains neutral with regard to jurisdictional claims in published maps and institutional affiliations.



This work is licensed under a Creative Commons Attribution 4.0 International License. The images or other third party material in this article are included in the article's Creative Commons license, unless indicated otherwise in the credit line; if the material is not included under the Creative Commons license, users will need to obtain permission from the license holder to reproduce the material. To view a copy of this license, visit <http://creativecommons.org/licenses/by/4.0/>

© The Author(s) 2016